







Assessment of prospective hazards resulting from the 2017 earthquake at the world heritage site Jiuzhaigou Valley, Sichuan, China


CHEN Xiao-qing^{1,2}  <http://orcid.org/0000-0002-0177-0811>; e-mail: xqchen@imde.ac.cn


CHEN Jian-gang^{1,3}  <http://orcid.org/0000-0001-6001-5413>; e-mail: chenjg@imde.ac.cn


CUI Peng^{1,2*}  <http://orcid.org/0000-0002-3973-5966>;  e-mail: pengcui@imde.ac.cn


YOU Yong¹  <http://orcid.org/0000-0001-7863-8686>; e-mail: yyong@imde.ac.cn

HU Kai-heng¹  <http://orcid.org/0000-0001-8114-5743>; e-mail: khhu@imde.ac.cn

YANG Zong-ji¹  <http://orcid.org/0000-0003-4108-2092>; e-mail: yzj@imde.ac.cn

ZHANG Wei-feng¹  <http://orcid.org/0000-0002-3333-7174>; e-mail: zwf@imde.ac.cn

LI Xin-po¹  <http://orcid.org/0000-0001-5876-057X>; e-mail: sinpore@126.com

WU Yong¹  <http://orcid.org/0000-0003-1370-7518>; e-mail: wuyong@imde.ac.cn

* Corresponding author

¹ Key Laboratory of Mountain Hazards and Earth Surface Process, Institute of Mountain Hazards and Environment, Chinese Academy of Sciences (CAS), Chengdu 610041, China

² CAS Center for Excellence in Tibetan Plateau Earth Sciences, Beijing 100101, China

³ Youth Innovation Promotion Association, CAS, Beijing 100029, China

Citation: Chen XQ, Chen JG, Cui P, et al. (2018) Assessment of prospective hazards resulting from the 2017 earthquake at the world heritage site Jiuzhaigou Valley, Sichuan, China. *Journal of Mountain Science* 15(4). <https://doi.org/10.1007/s11629-017-4785-1>

© Science Press, Institute of Mountain Hazards and Environment, CAS and Springer-Verlag GmbH Germany, part of Springer Nature 2018

Abstract: On August 8, 2017, a Ms = 7.0 magnitude earthquake occurred in the Jiuzhaigou Valley, in Sichuan Province, China (N: 33.20°, E: 103.82°). Jiuzhaigou Valley is an area recognized and listed as a world heritage site by UNESCO in 1992. Data analysis and field survey were conducted on the landslide, collapse, and debris flow gully, to assess the co-seismic geological hazards generated by the earthquake using an unmanned aerial vehicle (UAV), remote-sensing imaging, laser range finders, geological radars, and cameras. The results highlighted the occurrence of 13 landslides, 70

collapses, and 25 potential debris flow gullies following the earthquake. The hazards were classified on the basis of their size and the potential property loss attributable to them. Consequently, 14 large-scale hazards, 30 medium-sized hazards, and 64 small hazards accounting for 13%, 28%, and 59% of the total hazards, respectively, were identified. Based on the variation tendency of the geological hazards that ensued in areas affected by the Kanto earthquake (Japan), Chi-chi earthquake (Taiwan China), and Wenchuan earthquake (Sichuan China), the study predicts that, depending on the rain intensity cycle, the duration of geological hazard activities in the Jiuzhaigou Valley may last over ten years and will gradually decrease for the following five to ten years

Received: 4 December 2017

Revised: 19 January 2018

Accepted: 8 March 2018

before returning to pre-earthquake levels. Thus, necessary monitoring and early warning systems must be implemented to ensure the safety of residents, workers and tourists during the construction of engineering projects and reopening of scenic sites to the public.

Keywords: 2017 Jiuzhaigou earthquake; Disaster risk; Geological hazard; Landslide; World heritage site; Jiuzhaigou Valley

Introduction

UNESCO (UNESCO 2017) designated 1073 properties with outstanding universal value from 167 states as world heritage sites at the end of 2017. However, in recent years, world heritage properties have suffered extensive damage due to geological hazards such as earthquakes, landslides, volcanic eruptions, and tsunamis. Earthquakes and landslides have been recorded as the most frequent hazard type at world heritage sites (Pavlova et al. 2017; Cigna et al. 2018). For example, earthquakes devastated world heritage sites in Kathmandu

Valley, Nepal in 2015 (Fallahi 2015) and disrupted the Qiang people's watchtowers system in Sichuan, China in 2008 (Chen 2012). In addition, different types of landslides frequently occur on the slopes surrounding the affected properties and damage access roads and tourist paths to the sites (Wieczorek et al. 2007; Klimes 2013; Raso et al. 2014).

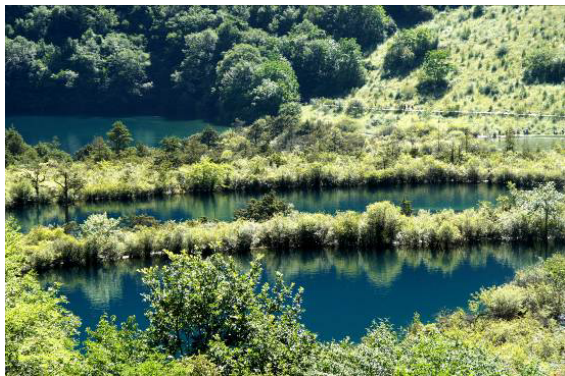
Jiuzhaigou Valley was recognized and listed as a world heritage by UNESCO in 1992. It includes 27 world heritage points that recognize its peculiar water landscape, variety of landform landscapes, and well-preserved glacial remains, some of them are shown in Figure 1. Unfortunately, on August 8, 2017, a $M_s = 7.0$ magnitude earthquake occurred in the Jiuzhaigou Valley (N: 33.20° , E: 103.82°). The earthquake affected a total of eight counties in Sichuan and Gansu Provinces. The maximum intensity of the earthquake reached nine degrees and the total area with intensity equal or greater than six degrees was 18,295 km². By 20:00 local time on August 13, 2017, the earthquake had killed 25 people, injured 525 people, and six people were missing. The earthquake affected 176,492 people



(a) Five Flower Lake



(b) Long Lake



(c) Shuzheng Lakes



(d) Nuorilang Waterfall

Figure 1 Photos of the world heritage points in Jiuzhaigou Valley before the earthquake.

(including tourists) and damaged 73,671 houses to varying degrees (including 76 collapsed houses). As shown in Figure 2, H stands for the elevation, 11 world heritage points were located in the nine-degree (IX) intensity range, including Jiuzhaigou town, Shuzheng Gully, Penjingtan, Dage Mountain, Sparking Lake, Shuzheng Lakes, Shuzheng Waterfall, Rhino Sea, Nuorilang Waterfall, Mirror Lake, and Pearl Beach. Additionally, 13 world heritage points in the eight-degree (VIII) intensity

area included Five Flower Lake, Panda Lake Waterfall, Rize Gully, Swan Sea, Sword Rock, Yangdong, Zharu Gully, Baojingyan, Zechawa Gully, Zhayizhaga Mountain, Semo Mountain, Ganzigonggai Mountain, and White River. Three world heritage points were located in the seven-degree intensity area, including the Five-color Pond, Long Lake, and Gaerna Mountain.

The aim of the present study is to provide qualitative information on geological hazards,

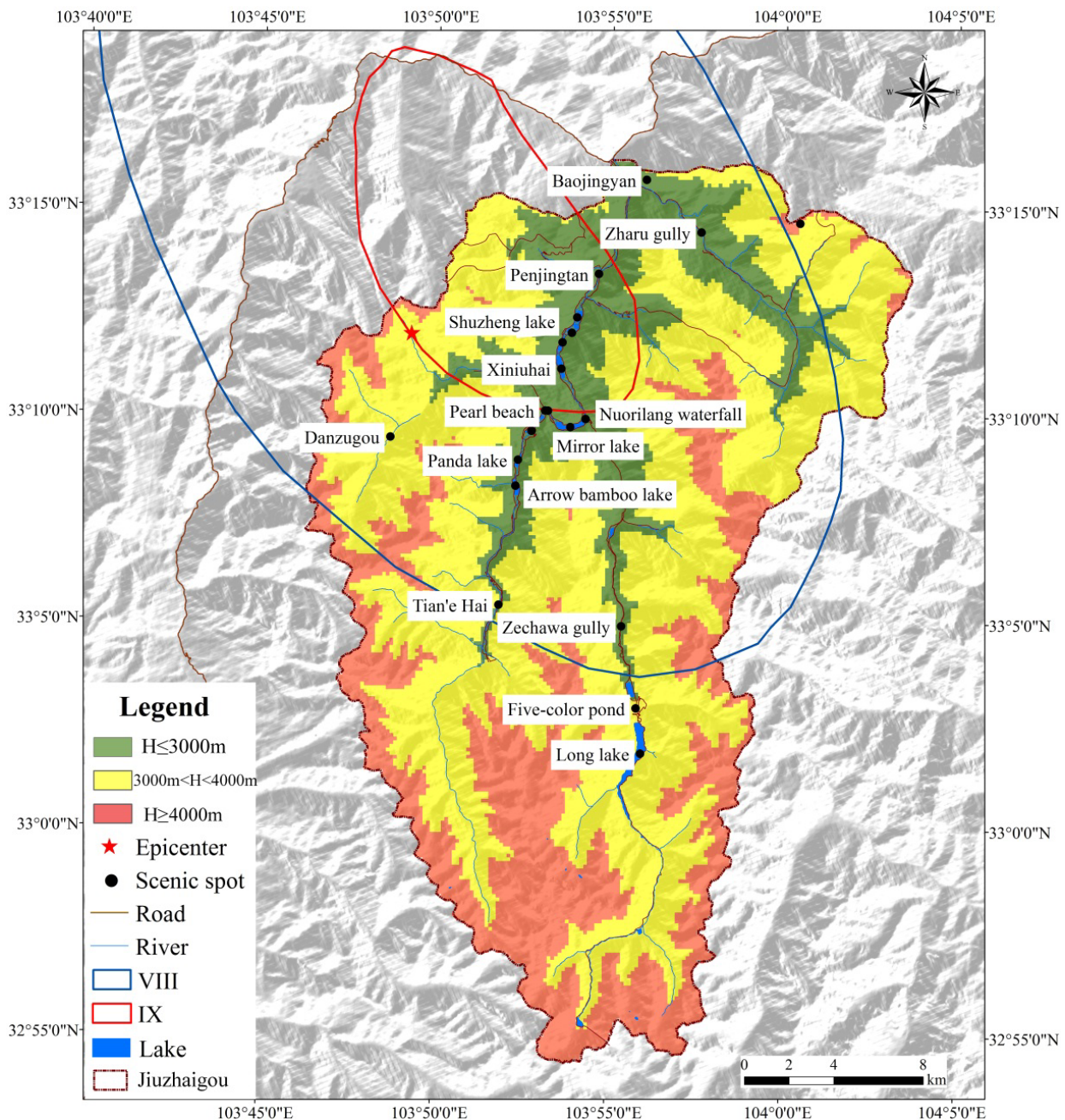


Figure 2 Location and elevation of Jiuzhaigou Valley and earthquake intensity.

including collapses, landslides, debris flows, and unstable slopes, generated by the 2017 Jiuzhaigou earthquake at the Jiuzhaigou Valley and highlight the risks of geological hazards to world heritage site managers. Firstly, types and distribution of geological hazards generated by the earthquake were analyzed. Secondly, the damage caused to roads, villages, landscape, and tourism facilities were assessed. Finally, trends in the variation of geological hazard activity were proposed based on the variation tendency of geological hazards in the areas affected by the Kanto earthquake (Japan), Chi-chi earthquake (Taiwan China), and Wenchuan earthquake (Sichuan China)..

1 Disaster Risk Factors at the Jiuzhaigou Valley

1.1 Geomorphologic conditions

The Jiuzhaigou Valley is located in the southeastern region of the Qinghai-Tibet Plateau in the transition zone from the Qinghai-Tibet Plateau to the Sichuan Basin, outside the mountainous area of the Sichuan Basin. The terrain of the park is higher in the south and lower in the north; maximum elevation of the Gaerna Mountain is 4764 m and the elevation of the outlet of Jiuzhaigou Valley is 1996 m, yielding a relative elevation difference of 2768 m. Based on their altitudes, the landforms at the Jiuzhaigou Valley can be divided into three categories: high-elevation mountains, high- and medium-elevation mountains, and medium-elevation mountains. The elevation boundary between the high-elevation and medium-high elevation mountains represents the altitude of the upper limit of the forest in the park and is 3800 m. The elevation boundary between the high- and medium-elevation mountains and the medium-elevation mountains represents the altitude of the lower limit of the coniferous forest belt in the park and measures 2800 m (Deng 2011).

1.2 Geological conditions

The Jiuzhaigou Valley lies on the edge of the subduction zone of the Qinghai-Tibet Plate and Yangtze Plate and the Songpan-Ganzi geosyncline area (Cui et al. 2005). The formation of the

Songpan-Ganzi geosyncline began in the Sinian, continued during the Permian, and ended at the end of the Triassic period. The exposed strata are Middle Devonian-Middle Triassic shallow marine to coastal carbonate sediments. The tectonic setting of the geosyncline is the Songpan-Ganzi orogenic belt, which is characterized by the convergent activity of the Danba-Wenchuan tectonic rocks and Motianling plots of the West Qinling orogenic belt. The eastern region of the geosyncline is the Longmen mountain fold belt, which is composed of Cathaysian and Neocathaysian structural systems; the Jiuzhaigou Valley is located in the northwestern region of the Motianling plots. Based on differences in its geologic evolution, sedimentary construction, metamorphism, and morphology, the park can be further divided into three structural units: the Tazang tectonic belt, Jiuzhaigou fold-thrust belt, and Nanping fold-thrust belt. Jiuzhaigou Valley is mainly located in the Jiuzhaigou fold-thrust belt.

1.3 Climate and hydrological conditions

1.3.1 Climatic characteristics

Precipitation is mainly concentrated from May to September, often in the form of rainstorms. The average annual precipitation in the Jiuzhaigou Valley at the Nuorilang Protection Station (elevation: 2380 m) is 646 mm. The annual change rate of precipitation is relatively small and ranges approximately from 10% to 15%. Precipitation is highest during summer (May to September), followed by autumn (October), and spring (from March to April). Lowest rainfall occurs during winter, which is from November to February of the following year (Cui et al. 2005). Rainfall records from 1984 to 2010 from the rain gauges distributed in the nine villages and the tourist center of Nuorilang were analyzed. During this period, the maximum monthly precipitation was 139.6 mm (July 2006) and minimum monthly precipitation was 0 mm (January 2006). Maximum daily rainfall of 24.2 mm was recorded on July 3, 2006, and maximum hourly rainfall of 8.6 mm was recorded on May 23, 2007. According to the temperature data obtained from the Nuorilang Protection Station, the average annual temperature was 7.3°C, average temperature of the hottest month (July)

was 16.8°C, and average temperature of the coldest month (January) was -8.7°C.

1.3.2 Hydrological characteristics

The Jiuzhaigou watershed extends over an area of 651.35 km² with 118 lakes in the main channel, covering a total area of 2.85 km². Its surface runoff is relatively stable and has low amplitude owing to high vegetation coverage. Surface runoff is mainly subject to atmospheric precipitation and groundwater recharge; in general, the runoff flows from south to north. The average discharge of the Yangdong River is 9.03 m³/s. Based on its distribution characteristics, the river flow discharge can be divided into wet season (from June to September), flat-water season (from April to May and October to November), and dry season (from December to March of the following year). Due to uneven distribution of precipitation during the year, the peak discharge of the downstream Baishui River exhibits bimodal characteristics and peaks mainly in July and September. The channel width of the Jiuzhaigou watershed is narrow and is less than 200 m. The maximum aspect ratio is 20:1, and the average aspect ratio is 4.5:1. The average gully slope with surface runoff is 38.7‰; the average gully slopes of Zechawa Gully and Rize Gully are 47.7‰ and 54.5‰, respectively, and the maximum average gully slope of Heijiao Gully is 225.2‰ (Cui et al. 2005).

2 Methodologies

Field surveys and measurements, remote-sensing imaging, laser range finders, and cameras were conducted on landslides, collapses, debris flow gullies, and unstable slopes to identify the locations and morphological characteristics of co-seismic geological hazards and determine the risk area following the Jiuzhaigou earthquake. An UAV (Inspire 2, DJI-Innovations, China) was utilized to detect scarps and take photos of the co-seismic landslides (Zhang et al. 2014; Erdelj et al. 2017). The remote sensing images (e.g. GF-1 with spatial resolution 2.0 m, TRIPLESAT with spatial resolution 0.8 m) and field photographs were used to determine the distribution and numbers of co-

seismic landslides associated with the Jiuzhaigou earthquake, and assess the amount of loose material in gullies, which can potentially form debris flows during rainfall. Landslides with minimum dimensions of 2 m were identified using the high resolution aerial photographs. This data was then integrated into maps highlighting debris flow source areas, flow paths, and flow deposits. This method has been successfully employed to study the geological hazard problems at other world heritage sites (Lollino and Audisio 2006; Margottini et al. 2015).

Field measurements with hand-held GPS and laser range finders (Contour XLRic, Contour company, USA) were conducted on geological hazard sites to determine their position and geological hazard range. The laser range finder had a maximum range of 1850 m with measurement accuracy of 0.10 m. A geological radar (model no, MALA GEOSCIENCE AB, Sweden), an economical and advanced test technology with characteristics of high resolution, accurate positioning, and speed (Zhao 2002) was used to measure the depth of the source material. Estimations of deposit areas and depths were based on field measurements and topographic maps. Deposit volumes were obtained by multiplying the observed depositional area with an estimated mean depth, which was obtained using the geological radar. The precision of this approach clearly depends on the accuracy of site-specific investigations and knowledge of the magnitude of geological hazard events (Zhang et al. 2014). Geomorphological considerations suggest that the measurement of deposit volume from actual field surveys was sufficiently accurate for the purpose of our work (Tang et al. 2012).

Types, volume, distribution, and extent of damage of geological hazards after the earthquake were assessed using aerial photographs taken before and after the earthquake. Field surveys were conducted on the ground using the UAV to verify the interpretations and completeness of mapping. Initiation sites were marked by fresh scouring, which were visible on the imagery and ground as a lighter tone than their surroundings, representing freshly exposed rock. In many co-seismic landslides, gullies and/or rills had developed, and were visible on the aerial photographs, aiding the identification process.

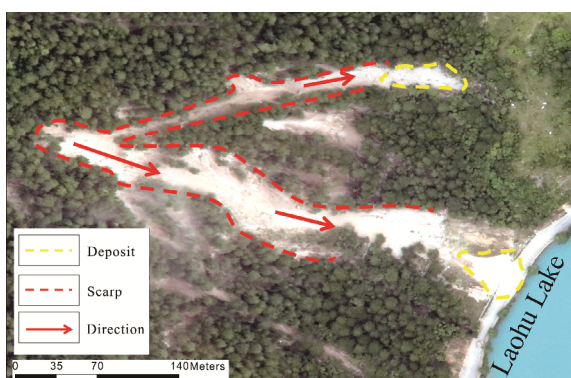
3 Types and Distribution of Geological Hazards Caused by the Jiuzhaigou Earthquake

3.1 Collapse

Collapse events are the most common and widely distributed events in the Jiuzhaigou Valley; they are characterized by multiple disaster points and the lithology of the collapsing material is dominated by calcareous and metamorphic rocks. Earthquake-induced collapse disasters were mainly distributed along the seismogenic fault of the

Jiuzhaigou Earthquake in the northwest direction, which can threaten vital lifelines such as the Laohu Lake and Zharu Gully.

The Laohu Lake collapse, as shown in Figure 3(a), was located at N: 103°53' and E: 33°11', at an altitude of 2288 m. The total volume of the collapse body was 11,000 m³ and the threatened area extended to nearly 3.95 × 10⁶ m². The maximum vertical fall height was 50 m and maximum horizontal fall distance was 50 m at the collapse point. The collapse possessed a loose structure and was comprised of gravel with diameters ranging from 0.02 m to 0.30 m. The Zharu Gully collapse



(a) Collapse on slope beside Laohu Lake



(b) Landslide near Pearl Beach and buried the tourist road



(c) Debris flow at Xiajijie lake in September 2017

Figure 3 Types of geological hazards caused by the Jiuzhaigou earthquake.

was located at N: 103°55' and E: 33°15'. The total volume of the collapse body was 12,100 m³ and the risk area extended over 3.34×10^6 m². The maximum fall height difference was 100 m and maximum fall distance was 80 m. The accumulation body of this collapse was characterized by loose structure and poor classification. The diameters of the fallen stones ranged from 0.02 m to 0.40 m.

3.2 Landslide

Small and medium-sized shallow landslides were dominant. The main types of landslides were soil landslides and rocky landslides and calcareous and metamorphic rocks dominated their lithologies. The earthquake-induced landslides were mostly concentrated along roads, and threatened the security of, and occasionally blocked roads. For example, nine medium or small landslides were detected along the road near the Mirror Lake; these landslides blocked the road upstream of the Mirror Lake and completely blocked road traffic upstream of the Five Flowers Lake, as shown in [Figure 3\(b\)](#). This landslide, located at N: 103°53' and E: 33°09', covered a total area of 2350 m², was 100 m in length, 50 m in width, up to 20 m in thickness, with an estimated volume of 25,000 m³. The elevation of the crown and toe were 2600 m and 2530 m, respectively, indicating that the height difference of the landslide was 70 m; the slope angle of the landslide body was 32°. The aspect of the landslide was NWW 290°. The exposed main scarp indicated that the landslide was a rocky landslide and the lithology of the exposed bed rock was carboniferous dolomite.

3.3 Debris flow

The debris flows in the Jiuzhaigou Valley exhibited the following characteristics. Firstly, the debris flow source areas were located at altitudes above 3800 m due to strong frost weathering. Secondly, debris flows were concentrated at the center of heavy rain activity. Thirdly, debris flows were predominantly distributed in previously forest cutting areas. Fourthly, debris flow activity ranged from 2000 m to 3000 m ([Cui et al. 2003 and 2007](#)).

Typical debris-flow gullies such as the

Shuzheng Gully and Xiajijie Lake have endangered villages and landscapes. Debris flows in Shuzheng Gully have significantly damaged Shuzheng village and Shuzheng Lake during previous events. Past debris flows have damaged Shuzheng village substantially and flowed into the Shuzheng Lake ([Cui et al. 2005](#)). In particular, from June to July 1988, three debris flows were triggered; the debris fan was located 200 m above the Shuzheng village and the debris flows moved downstream. Thus, if a large-scale debris flow is triggered, it could destroy Shuzheng village and Shuzheng Lakes and block tourist roads.

Pre-earthquake measurement of the watershed area of the Xiajijie Lake was 2.1 km²; main gully length was 2.5 km; and the mean channel slope was 612‰. An old debris fan was located at the gully outlet. The debris flows triggered by the 2017 earthquake exerted a scour effect on the fan, producing a scour channel with mean depth of 4.5 m, mean width of 11.5 m, and channel slope ranging from 268‰ to 380‰. Some collapses and landslides were noted along the gully; these solid materials acted as the source material for the debris flow. In this gully, three debris flows were triggered in 1976, 1983, and 1984; the debris flow in 1983 was the largest; the density ranged from 2100 kg/m³ to 2200 kg/m³, with maximum stone diameter of 3 m, and maximum debris flow discharge of 142 m³/s ([Cui et al. 2003; Cui et al. 2007](#)). After the 2017 Jiuzhaigou earthquake, four debris flows were triggered from September 14 to September 25, 2017, and about 15,000 m³ of solid materials were transported. These debris flows resulted in the burial of nearly 150 m of a long road and some of the debris flow materials poured into the Xiajijie Lake, shown in [Figure 3\(c\)](#), on September 25, 2017.

3.4 Distribution of earthquake-induced geological hazards

According to the size ([Jakob 2005; Hungr et al. 2014](#)) and potential property loss attributable to the earthquake-induced geological hazards, 14 large-scale, 30 medium-sized, and 64 small geological hazards, which accounted for 13%, 28%, and 59% of the total hazards, respectively, were identified. The distribution of earthquake-induced geological hazards appeared to be parallel to the

northwest-southeast strike-slip fault (Dai et al. 2017). The hazards were highly concentrated along the White River from Jiudaoguai to Jiuzhaigou Valley, especially in the Rize Gully from Tiger Mouth to Arrow Bamboo Lake, as shown in Figure 4. On-site investigations revealed the severe damage inflicted upon scenic spots, roads, facilities, water, and vegetation.

Based on the analysis results of the remote sensing images, the distances from the geological disaster points to the seismogenic fault were obtained. Among the 70 collapses, 39 collapses are located in distances less than 10 km and 89% of the collapses are located in distances less than 15 km. Moreover, 92% of the landslides and 84% of the potential debris flow gullies are located in distances less than 15 km, respectively. Furthermore, it is found that the number of the geological hazards decrease with increasing distance from the geological disaster point to the seismogenic fault. According to the results of the distribution of the

collapses and landslides in the Wenchuan Earthquake area, there are 9186 geological hazard spots of collapses and landslides were recognized, in which, 79% of the collapses and landslides were located in distances less than 15 km to the seismogenic fault (Huang 2009). These show a similar distribution trend of the earthquake-induced geological hazards. This trend was also verified by Xu and Li (2010) by analyzing 112 large scale landslides of Wenchuan earthquake with each area is large than $5 \times 10^4 \text{ m}^2$.

4 Damage Caused by Earthquake-induced Geological Hazards

4.1 Road damage

Overall, 76 secondary geological disasters, including collapses, landslides, and debris flows, severely destroyed the tourist roads after the

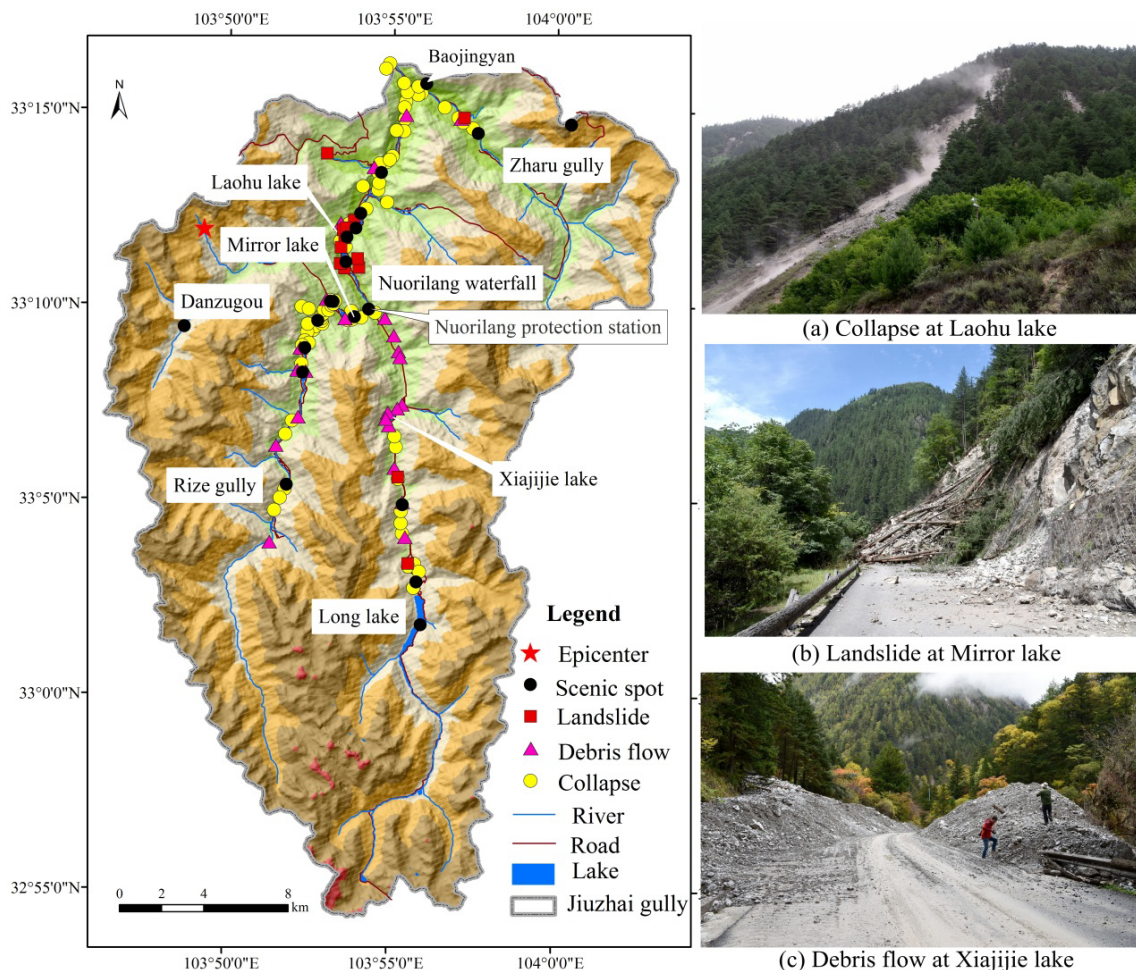


Figure 4 Distribution of 2017 Jiuzhaigou earthquake-induced geological hazards in Jiuzhaigou Valley.

earthquake, as illustrated in Figure 5. These have been manifested in three modes: (a) original tourist roads were deformed or partially collapsed. For example, the tourist roads on the right bank of the Mirror Lake were affected by unstable slope deformation. Cracks nearly 200 m to 300 m in length, 0.01 m to 0.30 m in width, and 0.01 m to 0.80 m in height, were observed on this road. (b) Geological disasters caused partial landslide deformation in some sections of the roads. For example, two landslide deformation events caused by unstable slopes occurred on roads on the right bank of the Mirror Lake. (c) Due to collapses, landslides, and deformation of unstable slopes, tourist roads were buried or blocked. Collapses in the inner sections of roads resulted in fragmentary sliding or collapse, which affected road safety.

4.2 Potential risk to the community

Eight hazard spots that threatened scattered villages and inhabited districts, including three spots in the Heye community, two in the Zharu community, two in the Shuzheng community, and one in the Zechawa community, were identified.

These communities were located in the danger zone of geological hazards and were vulnerable to landslides, collapses, and debris flows, such as the landslide in Zharu Gully. Additionally, unstable deformation blocked channels resulting in varying degrees of damage, such as the collapse that occurred behind the Zharu Temple. As shown in Figure 6(a), Zharu village is located on a debris-flow fan. Some hazard mitigation structures were constructed in the gully before the earthquake, but after the earthquake, the amount of loose earth increased, much of it due to the occurrence of many collapses and landslides in the gully. We deduce that the risk of debris flow disaster increases with the strong rainfall. The potential risk area of the debris flow hazard is evaluated to be $55 \times 10^4 \text{ m}^2$ and 134 local people living in this area are threatened. Moreover, a landslide with risk area of $5 \times 10^4 \text{ m}^2$ is located opposite Zharu village on the left bank of the river; it has the potential risk of blocking the river.

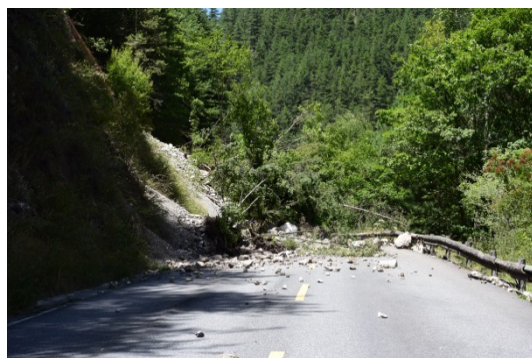
Figure 6(b) shows the Heye community, which is exposed to risks of collapses, landslides, and debris flows. Before the 2017 Jiuzhaigou earthquake, seven debris-flow check dams were



(a) Road-surface damage



(b) The subgrade damage



(c) Landslide blocked the road



(d) Debris flow blocked the road

Figure 5 Tourist road damage caused by 2017 Jiuzhaigou earthquake-induced geological hazards.



(a) Zharu village



(b) Heye village

Figure 6 Potential risk caused by 2017 Jiuzhaigou earthquake-induced geological hazards in Zharu village and Heye village.

constructed in 1991 and a debris-flow blocking system was implemented. After the earthquake, active and passive protective measures against collapses were implemented to protect the

residents. However, under the double effect of the earthquake and engineering design limitations, large-scale debris flows can be triggered by strong rain storms, indicating that the potential risk to the

Heye community is high. After the earthquake, two large collapses occurred around the community and the potential debris flow volume was increased. The total volume of the collapse around the community is estimated to be $13.1 \times 10^4 \text{ m}^3$ and the risk area is $5.6 \times 10^4 \text{ m}^2$. The potential risk area of the debris flow hazard is $25 \times 10^4 \text{ m}^2$ and about 452 local people living in this area are threatened. Moreover, the traffic road and the scenic spot near the community are also in the risk area.

4.3 Damage to the landscape and tourism facilities

Thirteen disaster points that threaten the landscape in Jiuzhaigou Valley have been identified. The threat posed by geological hazards to the landscape is based on the following facts: (a) some landscapes are located in danger zones and can be destroyed if a disaster is triggered. (b) Some collapses and unstable slopes with obvious deformations can severely impair vegetation and natural landscape.

The Panda Lake is located at an elevation of 2587 m, with depth of 14 m and an area of $9 \times 10^4 \text{ m}^2$. Figure 7(a) illustrates the situation at the Panda Lake after the earthquake. The surface area of Panda Lake was affected by the collapse and landslide, which slipped into the lake. The clarity of the water became cloudy. Around the Panda Lake, the collapse volume is totally $8.43 \times 10^5 \text{ m}^3$ and the risk area is $1.94 \times 10^6 \text{ m}^2$. Sparking Lake is downstream from Panda Lake, located 2211 m above sea level, 232 m long, 134-294 m wide, and 16 m deep, with a total capacity of $45 \times 10^4 \text{ m}^3$. Following the earthquake, the dam of Sparking Lake was broken and a dam failure breach was formed, which was 40 m long, 12 m wide, and 15 m deep. All the water flowed into the downstream lakes of the Sparking Lake and the completely destroyed Sparking Lake was shown in Figure 7(b).

Seven disaster points threatened the tourist facilities in the Jiuzhaigou Valley. Most of the damage to tourism facilities was caused by collapse in this area and a small number of facilities were seriously damaged by the debris flow and outbreak



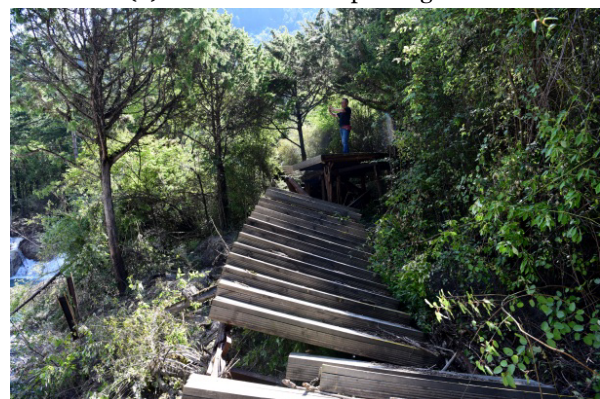
(a) Panda lake affected by landslide and collapse



(b) Outbreak of the Sparking lake



(c) Damaged tourist facilities by debris flow



(d) Damaged tourist facilities by outburst flood

Figure 7 The landscape and tourism facilities damaged by Jiuzhaigou earthquake on Aug. 8, 2017.

flood, such as the plank walk, as shown in [Figure 7\(c\) and \(d\)](#). The risk area of the debris flow in the Zechawa gully is 5×10^4 m² and the plank walk located in the debris-flow accumulation area will be damaged after a large-scale debris flow. After the dam failure of the Sparking Lake, a nearly 900 m long plank walk was washed away by the outbreak flood. Additionally, 53 geological hazards threatened water bodies. Vegetation was severely impaired by landslides, collapses, and deformation of unstable slopes. These hazards can destroy the landscape and affect its outstanding universal value. Further, these hazards may aggravate soil erosion and affect the downstream landscape area and water bodies and cause serious damage to the original forestland.

5 Variation Trends of Post-earthquake Geo-hazard Activities

Preliminary investigation conducted on August 25, 2017 revealed that the number, scale, and potential danger level of geological disasters have notably increased following the earthquake. Landslides, collapses, and debris flows were the main types of geological disasters. Most of the earthquake-induced geological disasters in the Jiuzhaigou Valley were small and medium-sized, and accounted for 87% of the 108 disaster points. The number of major geological hazards rapidly increased, which significantly increased the degree of harm.

In addition, as the Jiuzhaigou Valley is located in an area containing numerous intersecting fault zones, the 2008 Wenchuan earthquake had also exerted some impact on this region. Due to the influence of multiple earthquakes, secondary geological disasters in the Jiuzhaigou earthquake-stricken area are mainly characterized as long-term, complex, and concealed disasters. In earthquake-stricken areas, rocky soils are damaged and potentially unstable slopes and shaky mountains are covered by abundant vegetation, which are mainly concentrated at high elevations where they are well-concealed. Therefore, secondary geological disasters are difficult to find, monitor, and mitigate. These potentially unstable slopes are likely to be destroyed and cause significant damage, as witnessed during the Zhongxing town landslide on

July 10, 2013, Dujiangyan City, China ([Yin et al. 2016](#); [Chen and Cui 2017](#)) and Xinmo village landslide on June 24, 2017, Maoxian Country, China ([Su et al. 2017](#)).

Therefore, it is necessary to systematically study potential large-scale geological disasters in earthquake-stricken areas. Detailed geological surveys, disaster identification, and risk evaluation of potential disasters for important communities, landscapes, and infrastructure should be conducted and corresponding risk management and coping strategies should be proposed. [Huang \(2011\)](#) proposed that the evolution model of the post-earthquake geological disasters were mainly from the Kanto earthquake in Japan (1923) and the Chi-chi earthquake in China (1999). Based on the secondary mountain disasters that occurred in areas affected by the Kanto earthquake, Chi-Chi earthquake, and Wenchuan earthquake, the duration of geological hazard activity is expected to last approximately ten years and may gradually decrease for the next five to ten years (i.e., the rainstorm cycle) before returning to pre-earthquake levels ([Koi et al. 2008](#); [Hu et al. 2010](#); [Inoue 2011](#); [Chen et al. 2015](#); [Chiou et al. 2007](#); [Cui et al. 2011](#); [Fang et al. 2012](#); [Ge et al. 2015](#)).

The outbreak risk of collapses, landslides, and debris flows is high, and these disasters have the highest degree of potential harm. Moreover, the risk of geological disasters is also high. Thus, survey, monitoring, and prevention of geological disasters should increase during the flood season. Monitoring, early warning, and engineering-based mitigation of geological disasters should be strengthened after an earthquake especially in Heye village, Shuzheng village, Zharu village, and Zechawa village and important attractions in the Jiuzhaigou Valley. Due to the particular features of the natural landscape, engineering and non-engineering measures used for prevention and mitigation of geological disasters in the valley must be coordinated with the landscape. Therefore, post-disaster reconstruction work is very difficult; the organic combination of scientific research and reconstruction must be strengthened, and engineering and biological measures must also be harmoniously combined ([Zvelebil and Moser 2001](#); [Gerald et al. 2007](#); [Chiara et al. 2013](#)). In addition, as prevention and control of geological disasters is related to the safe passage of traffic, reconstruction

must prioritize on disaster mitigation and road safety.

6 Conclusions and Recommendation

(1) Totally, 108 earthquake-induced geological hazards were identified in the Jiuzhaigou Valley, including 70 collapses, 13 landslides, and 25 potential debris flow gullies, wherein small and medium-sized hazards accounted for 87% of the total sites. Furthermore, collapses and landslides resulting from earthquakes have produced loose soils and strong disturbances of the earth's surface in this area and have seriously damaged the vegetation. These altered surroundings are conducive to the formation of large-scale debris flows during rainfall events, especially extreme rainstorms.

(2) Risk will be higher when collapses, landslides, and debris flows occur intensively during tectonic activity. Therefore, monitoring and early warning systems should be urgently established. Moreover, an integrated disaster mitigation plan should be devised as soon as

possible. Engineering countermeasures and non-structural measures should be coordinated with landscape characteristics to design a disaster mitigation strategy, which will specifically address the characteristics of the Jiuzhaigou Valley.

(3) Based on the variation tendency of geological hazards in areas affected by the Kanto earthquake, Chi-chi earthquake, and Wenchuan earthquake, the duration of geological hazard activity may last for ten years and may gradually decline for the next five to ten years (i.e., the rainstorm cycle) before returning to pre-earthquake levels. Thus, during the construction of engineering projects and reopening of scenic sites, necessary monitoring and early warning systems must be functional to ensure the safety of tourists and workers.

Acknowledgment

This study was supported by the National Science Foundation of China (Grant No. 41790432) and the International partnership program of CAS (Grant No. 131551KYSB20160002).

References

- Chen T (2012) The rescue, conservation, and restoration of heritage sites in the ethnic minority areas ravaged by the Wenchuan earthquake. *Frontiers of Architectural Research* 1(1): 77-85. <https://doi.org/10.1016/j.foar.2012.02.006>
- Chen XC, Cui YF (2017) The formation of the Wulipo landslide and the resulting debris flow in Dujiangyan City, China. *Journal of Mountain Science* 14: 1100-1112. <https://doi.org/10.1007/s11629-017-4392-1>
- Chen XQ, Cui P, You Y, et al. (2015) Engineering measures for debris flow hazard mitigation in the Wenchuan earthquake area. *Engineering Geology* 194: 73-85. <https://doi.org/10.1016/j.enggeo.2014.10.002>
- Chiara C, Giorgio P, Shahina T, Maria T (2013) First steps towards a landslide inventory map of the Central Karakoram National Park. *European Journal of Remote Sensing* 46(1): 272-287. <https://doi.org/10.5721/EuJRS20134615>
- Chiou SJ, Cheng CT, Hsu SM, et al. (2007) Evaluating landslides and sediment yields induced by the Chi-Chi earthquake and heavy rainfalls. *Journal of Geoenvironment* 2(2): 73-82. [https://doi.org/10.6310/jog.2007.2\(2\).4](https://doi.org/10.6310/jog.2007.2(2).4)
- Cigna F, Tapere D, Lee K (2018) Geological hazards in the UNESCO World Heritage sites of the UK: From the global to the local scale perspective. *Earth-Science Reviews* 176: 166-194. <https://doi.org/10.1016/j.earscirev.2017.09.016>
- Cui P, Chen XQ, Liu SQ, et al. (2007) Techniques of debris flow prevention in national parks. *Earth Science Frontiers* 14(6): 172-180. [https://doi.org/10.1016/S1872-5791\(08\)60009-3](https://doi.org/10.1016/S1872-5791(08)60009-3)
- Cui P, Chen XQ, Zhu YY, et al. (2011) The Wenchuan Earthquake (May 12, 2008), Sichuan Province, China, and resulting geological hazards. *Natural Hazards* 56: 19-36. <https://doi.org/10.1007/s11069-009-9392-1>
- Cui P, Liu SQ, Tang BX, et al. (2003) Prevention mode of debris flow in national parks: taking the world natural heritage (Jiuzhaigou) as an example. *Science in China Ser. E Technological Sciences* 2003: 33(Sup): 1-9. (In Chinese)
- Cui P, Liu SQ, Tang BX, et al. (2005) *Research and Prevention of Debris Flow in National Parks*. Beijing: Science Press. (In Chinese)
- Dai LX, Xu Q, Fan XM, et al. (2017). A preliminary study on spatial distribution patterns of landslides triggered by Jiuzhaigou earthquake in Sichuan on August 8th, 2017 and their susceptibility assessment. *Journal of Engineering Geology* 25(4): 1151-1164.
- Deng GP. (2011) Study of tourism geosciences landscape formation and protection of Jiuzhaigou world natural heritage site. PhD thesis. Chengdu University of Technology. (In Chinese)
- Erdelj M, Król M, Natalizio E (2017) Wireless Sensor Networks and Multi-UAV systems for natural disaster management. *Computer Networks* 124 (2017) 72-86. <https://doi.org/10.1016/j.comnet.2017.05.021>
- Fallahi A (2015) National Planning Commission, Nepal Earthquake 2015. Post Disaster Needs Assessment, Government of Nepal, National Planning Commission, Singha.
- Fang H, Cui P, Pei LZ, et al. (2012) Model testing on rainfall-induced landslide of loose soil in Wenchuan earthquake region. *Natural Hazards and Earth System Science* 12: 527-533. <https://doi.org/10.5194/nhess-12-527-2012>

- Ge YG, Cui P, Zhang JQ, et al. (2015) Catastrophic debris flows on July 10th 2013 along the Min River in areas seriously-hit by the Wenchuan earthquake. *Journal of Mountain Science* 12(1): 186-206. <https://doi.org/10.1007/s11629-014-3100-7>
- Gerald F, Wieczorek EL, Geist RJ, Motyka MJ (2007) Hazard assessment of the Tidal Inlet landslide and potential subsequent tsunami, Glacier Bay National Park, Alaska. *Landslides* 4: 205-215. <https://doi.org/10.1007/s10346-007-0084-1>
- Hu KH, Cui P, Wang CC, et al. (2010) Characteristic rainfall for warning of debris flows. *Journal of Mountain Science* 7: 207-214. <https://doi.org/10.1007/s11629-010-2022-2>
- Huang RQ (2009) Geohazard assessment of the Wenchuan earthquake. Science Press, Beijing, China. (In Chinese)
- Huang RQ (2011) After effect of geohazards induced by the Wenchuan earthquake. *Journal of Engineering Geology* 19(2): 145-151. (In Chinese)
- Hungr O, Leroueil S, Picarelli L (2014) The Varnes classification of landslide types, an update. *Landslides* 11: 167-194. <https://doi.org/10.1007/s10346-013-0436-y>
- Inoue K (2001) The Kanto Earthquake (1923) and sediment disasters. *The Earth Monthly* 23: 147-154. (In Japanese)
- Jakob M (2005) A size classification for debris flows. *Engineering Geology* 79: 151-161. <https://doi.org/10.1016/j.enggeo.2005.01.006>
- Klimes J (2013) Landslide temporal analysis and susceptibility assessment as bases for landslide mitigation, Machu Picchu, Peru. *Environmental Earth Science* 70: 913-925. <https://doi.org/10.1007/s12665-012-2181-2>
- Koi T, Hotta N, Ishigaki I, et al. Prolonged impact of earthquake-induced landslides on sediment yield in a mountain watershed: The Tanzawa region, Japan. *Geomorphology* 101: 692-702. <https://doi.org/10.1016/j.geomorph.2008.03.007>
- Lollino G, Audisio C (2006) UNESCO World Heritage sites in Italy affected by geological problems, specifically landslide and flood hazard. *Landslides* 3(4): 311-321. <https://doi.org/10.1007/s10346-006-0059-7>
- Margottini C, Fidolini F, Iadanza C, et al. (2015) The conservation of the Shahr-e-Zohak archaeological site (central Afghanistan): Geomorphological processes and ecosystem-based mitigation. *Geomorphology* 239: 73-90. <https://doi.org/10.1016/j.geomorph.2014.12.047>
- Pavlova I, Makarigakis A, Depret T, et al. (2017) Global overview of the geological hazard exposure and disaster risk awareness at world heritage sites. *Journal of Cultural Heritage* 28:151-157. <https://doi.org/10.1016/j.culher.2015.11.001>
- Raso E, Faccini F, Firpo M, et al. (2014) Rockfall hazard analysis and prevention in the middle-eastern sector of the Cinque Terre area (Italy). In: Abstract, 17th Joint Geomorphological Meeting in Liege, Belgium.
- Su LJ, Hu KH, Zhang WF, et al. (2017) Characteristics and triggering mechanism of Xinmo landslide on 24 June 2017 in Sichuan, China. *Journal of Mountain Science* 14: 1689-1700. <https://doi.org/10.1007/s11629-017-4609-3>
- Tang C, Asch TWJV, Chang M, et al. (2012) Catastrophic debris flows on 13 August 2010 in the Qingping area, southwestern China: The combined effects of a strong earthquake and subsequent rainstorms. *Geomorphology* 139-140: 559-576. <https://doi.org/10.1016/j.geomorph.2011.12.021>
- UNESCO, 2017. World Heritage list. Available on: <http://whc.unesco.org/en/list/>, accessed on 8 December 2017.
- Wieczorek GF, Geist EL, Motyka RJ, et al. (2007) Hazard assessment of the Tidal Inlet landslide and potential subsequent tsunami, Glacier Bay National Park, Alaska. *Landslides* 4: 205-215. <https://doi.org/10.1007/s10346-007-0084-1>
- Xu Q, Li WL (2010) Distribution of large-scale landslides induced by the Wenchuan Earthquake. *Journal of Engineering Geology* 18(6): 818-826. (In Chinese)
- Yin YP, Cheng YL, Liang JT, et al. (2016) Heavy-rainfall-induced catastrophic rockslide-debris flow at Sanxicun, Dujiangyan, after the Wenchuan Ms 8.0 earthquake. *Landslides* 13: 9-23. <https://doi.org/10.1007/s10346-015-0554-9>
- Zhang YS, Cheng YL, Yin YP, et al. (2014) High-position debris flow: A long-term active geological hazard after the Wenchuan earthquake. *Engineering Geology* 180: 45-54. <https://doi.org/10.1016/j.enggeo.2014.05.014>
- Zhao ZH. (2002) The application of ground penetrating radar to the investigation of geologic hazard. *The Chinese Journal of Geological Hazard and Control* 13(2): 100-102. (In Chinese)
- Zvelebil J, Moser M (2001) Monitoring based time-prediction of rock falls: three case-histories. *Physics and Chemistry of the Earth, Part B: Hydrology, Oceans and Atmosphere* 26: 159-167. [https://doi.org/10.1016/S1464-1909\(00\)00234-3](https://doi.org/10.1016/S1464-1909(00)00234-3)